Supplement of

Molecular Characteristics of Organosulfur Compounds in Guangzhou, South China: Heterogeneous Secondary Reactions Drivers the Molecular Distribution"

Hongxing Jiang et al.,

Correspondence to:Jun Li (junli@gig.ac.cn)

Supplementary text

Measurements for particulate total sulfur and water-soluble sulfate

About 1~3 pieces of filters were cut using the steel punchers (1.5 cm^2) and then put it into clean tin boats directly. The sample were then crashed into a ball and further analyzed using elemental analyzer (Germany, elementar unicube) coupled with high sensitivity thermal conductivity detector in the CNS mode. The particle sulfur in $PM_{2.5}$ samples were calculated according to the calibration curve which were obtained by analyzing standard samples with different mass. The water-soluble sulfate or SO_4^{2-} was analyzed with ion-chromatography (761 Compact IC, Metrohm, Switzerland). Detailed information about the analysis procedures were described in our previous studies (Jiang et al., 2020; Jiang et al., 2021b). Anions were separated on a Metrohm Metrosep A sup5-250 column with 3.2 mM Na_2CO_3 and 1.0 mM $NaHCO_3$ as the eluent and 35 mM H_2SO_4 for a suppressor. The injection loop volume for anion was 100 μL. The water-soluble sulfate-sulfur was calculated as 1/3 of the SO_4^{2-} concentration.

Operating conditions for FT-ICR MS analysis

The ultrahigh-resolution FT-ICR-MS enables identification of complex atmospheric mixtures by giving accurate m/z value, and each peak was assigned to an ambiguous formula with <1ppm absolute mass error was achieved (Jiang et al., 2021a). Previous study has indicated that the OSs are readily ionized in the negative ESI mode, and most of them were observed only in the negative mode (Lin et al., 2012b; Kuang et al., 2016). Therefore, the negative ESI FT-ICR-MS analysis could provide a comprehensive understanding about the chemical composition of organosulfur compounds (OSCs) in atmosphere, though the molecular structures such as potential isomers were generally hidden behind a given m/z value.

A total of 55 $PM_{2.5}$ samples were used for negative ESI-FT-ICR MS analysis and each sample were ultrasonic extracted with methanol in cold water bath (Jiang et al., 2021a). The methanol extracts were filtered with PTFE members and concentrated, and direct injected into a 9.4T solariX XR FT-ICR mass spectrometer (Bruker Daltonik GmbH, Bremen, Germany) in negative ESI modes at a flow rate of 180 mL h^{-1} (Jiang et al., 2021a; Jiang et al., 2020). Detailed operating conditions are set as: capillary voltage and capillary column end voltage for the negative ESI-FT-ICR MS analysis were set to 4.5 kV and -500 V, ions were accumulated in a hexapole for 0.65s, and the conditions of Octupole were set as 5 MHz and 350 V of peak to-peak (Vp-p) radio frequency (RF) amplitude. An argon-filled hexapole collision pool was operated at 2 MHz and RF amplitude of 1400 Vp-p, in which ions were accumulated for 0.02 s. The optimized mass for quadrupole (Q1) was 170 Da with the time of flight is 0.65ms. The mass range was set as150–800 Da, and a total of 128 continuous 4M data FT-ICR transients were co-added to enhance the signal-to-noise ratio and dynamic range. Field blank filters were processed and analyzed following the same procedure to detect possible contamination. The mass spectra were calibrated externally with arginine clusters in negative ion mode using a linear calibration. The final spectrum was internally recalibrated with typical O_2 class species peaks using quadratic calibration in DataAnalysis 5.0 (Bruker Daltonics). A typical mass-resolving power (m/Δm50 %,

in which Δm50% is the magnitude of the mass spectral peak full width at half-maximum peak height) >450 000 at m/z 319 with <0.3 ppm absolute mass error was achieved.

FT-ICR MS data processing

A custom software was used to calculate all mathematically possible formulas for all ions with a signal-to-noise ratio above 4 using a mass tolerance of ±1ppm. The compounds assigned as $C_cH_hO_oN_nS_s$ with s = 1, 2 will be collectively referred to as organosulfur compounds (OSs) including CHOS (n = 0) and CHONS (n = 1,2). The identified formulas containing isotopomers (i.e., ^{13}C, ^{18}O or ^{34}S) was not discussed. The intensity-weighted elemental ratios such as O/C, H/C, O/S were calculated as described in previous study (Jiang et al., 2021a). The double bond equivalent (DBE) is calculated using the equation:

$$DBE = (2c+2-h+n)/2.$$

Additionally, the modified index of aromaticity equivalent (Xc) which was considered as a better index to describe potential monocyclic and polycyclic aromatic compounds with S atoms, were also calculated using the flowing equation (Ye et al., 2020; Yassine et al., 2014):

$$X_c = \frac{3[DBE - (m \times o + n \times s)] - 2}{DBE - (m \times o + n \times s)}$$

Where m and n correspond to the fraction of oxygen and sulfur involved in the π-bond structure of the compound, respectively. If DBE ≤ (m×o+n×s), then Xc=0 is assumed. For chemical classes including alchohol, ether, sulfide, disulfide, sulfinic and sulfonic acids, m=n=0 should be used. And for chemical classes including carboxylic acid, ester and nitro, m=0.5 was adopted. Assuming the sulfur atom of organosulfur molecule exists in a sulfate group (R-OSO_3H) or a sulfonate group (R-SO_3H), the organosulfur molecule can be converted into a virtual organic carbon molecule by replacing -OSO_3H with -OH (or -SO_3H with -H). Considering negative ESI-FT-ICR MS analysis was performed, and the negative ESI mode is sensitive to compounds containing carboxylate, sulfonate and nitro groups. Thus, the calculation for Xc of organosulfur compounds can be simplified as (Ye et al., 2020):

$$X_c = \frac{3[DBE - 0.5 \times (o - 4)] - 2}{DBE - 0.5 \times (o - 4)}$$

We rounded 0.5×(*o*–4) down to the next lower integer if *o* is an odd number. A value of Xc≥2.5000 was supposed as the unambiguous minimum criterion for the presence of an aromatic structure. Xc≥2.7143, 2.8000, 2.8333, 2.9231 were considered as the thresholds for molecules containing cores of naphthalene, anthracene, pyrene and ovalene, respectively.

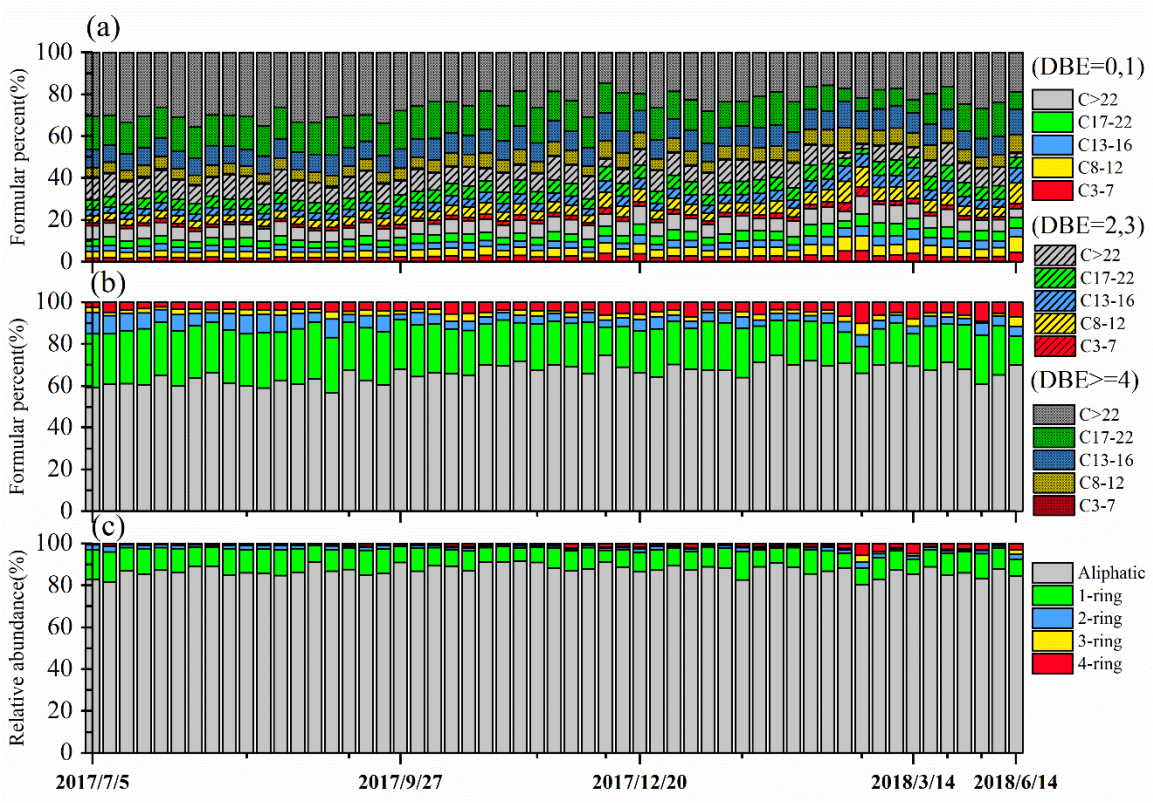

Figure S1. (a) Formular number percentages of each subgroup which divided based on the DBE value and the length of carbon skeleton in the formulas; (b) and (c) Relative abundance and formular number percentages of each subgroup which divided based on the Xc value of formulas.

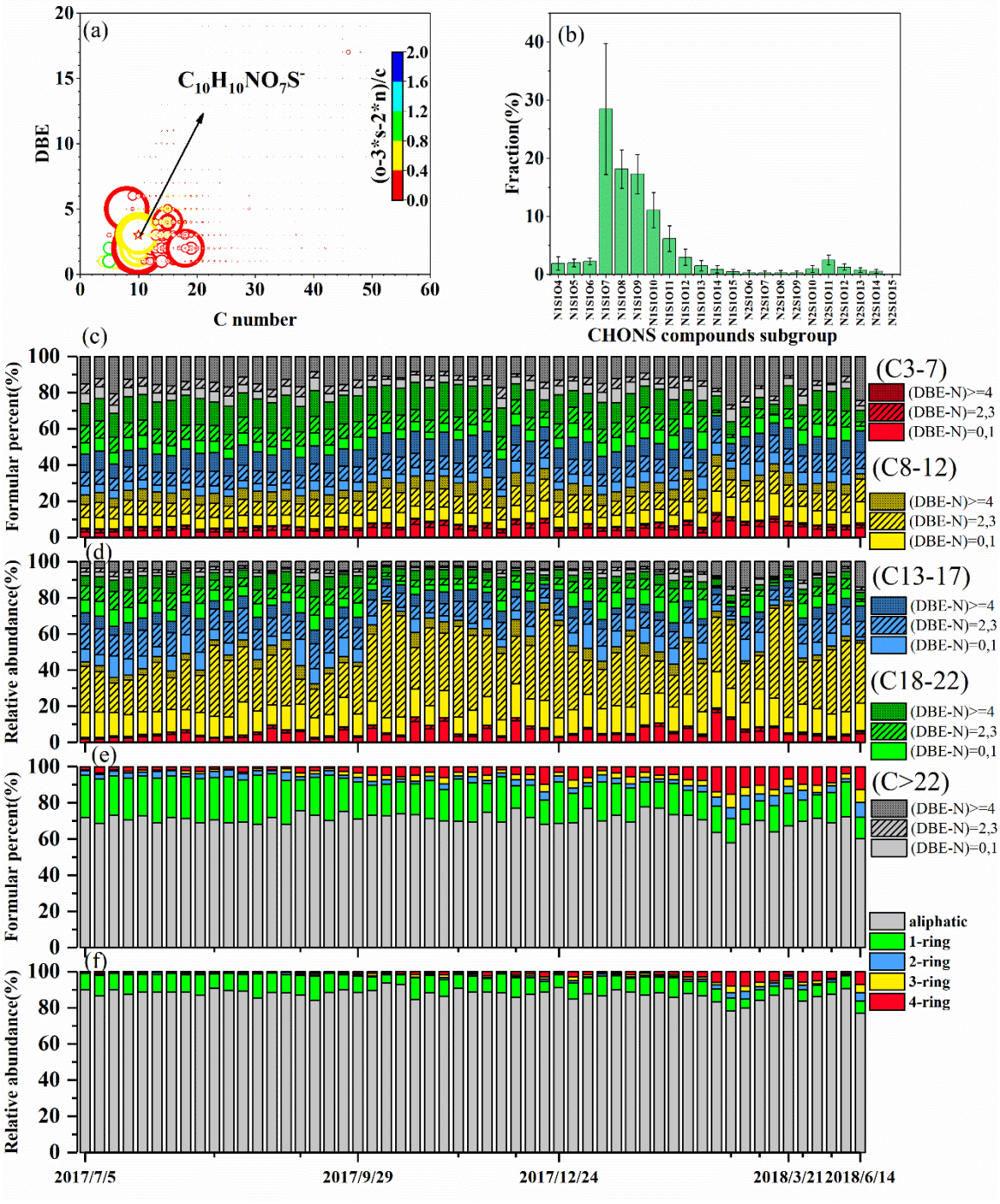

Figure S2. Molecular distribution of CHONS compounds detected by FT-ICR MS for the sample set collected in Guangzhou. (a) Double bond equivalent (DBE) vs C number for all the CHONS compounds of all samples. The color bar and marker size denote the number of oxidation state and the average sum-normalized relative peak intensities of the compounds; (b) Classification of CHONS species into different subgroups according to the numbers of S and O atoms in their molecules; (c) and () Relative abundance and formular number percentages of each subgroup which divided based on the DBE value and the length of

carbon skeleton in the formulas; (e) and (f) Relative abundance and formular number percentages of each subgroup which divided based on the Xc value of formulas.

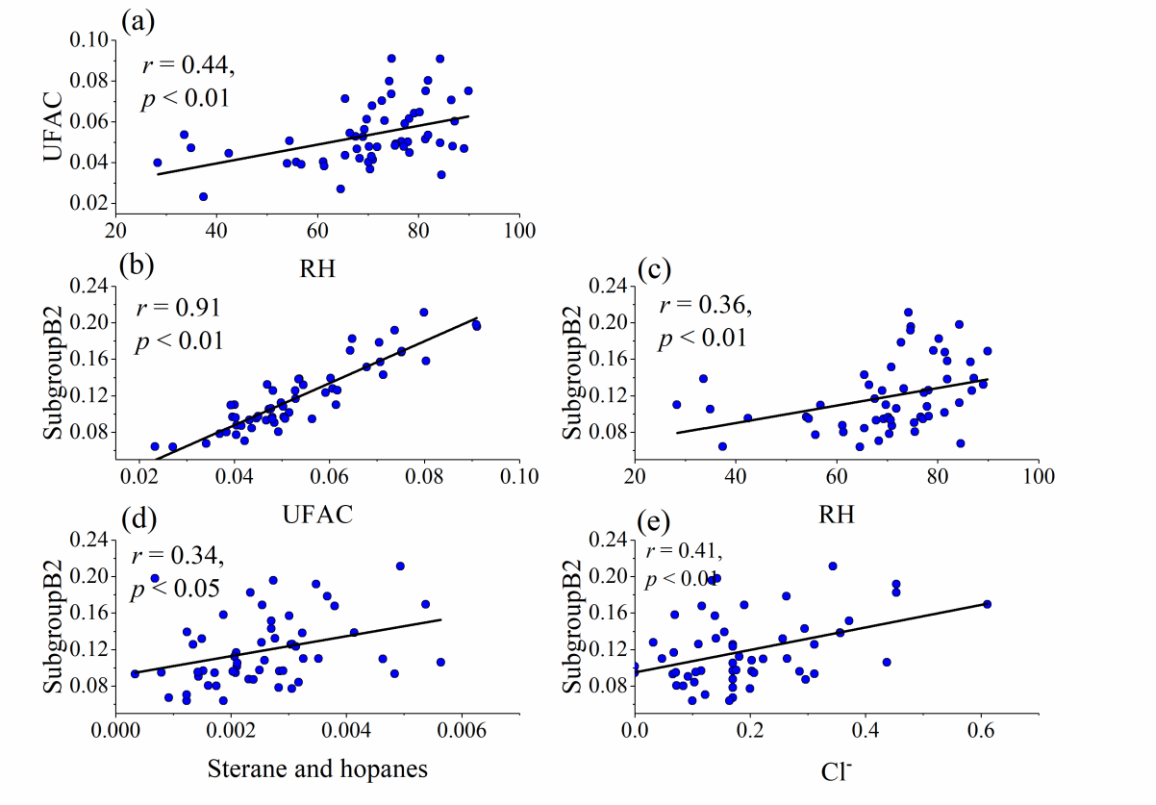

Figure S3. Significant correlations between (a) the sum-normalized intensity of OSs form potential unsaturated fatty acid compounds (UFAC) and RH, and the sum-normalized intensity of OSs classified into the subgroupB2 (with DBE≤2, C > 8, 3<O<7 for CHOS and DBE≤2, N=1, C > 8, 6<O<10 for CHONS compounds) and (b) UFAC, (c) RH, the concentrations of (d) sterane and hopanes, (e) Cl^-.

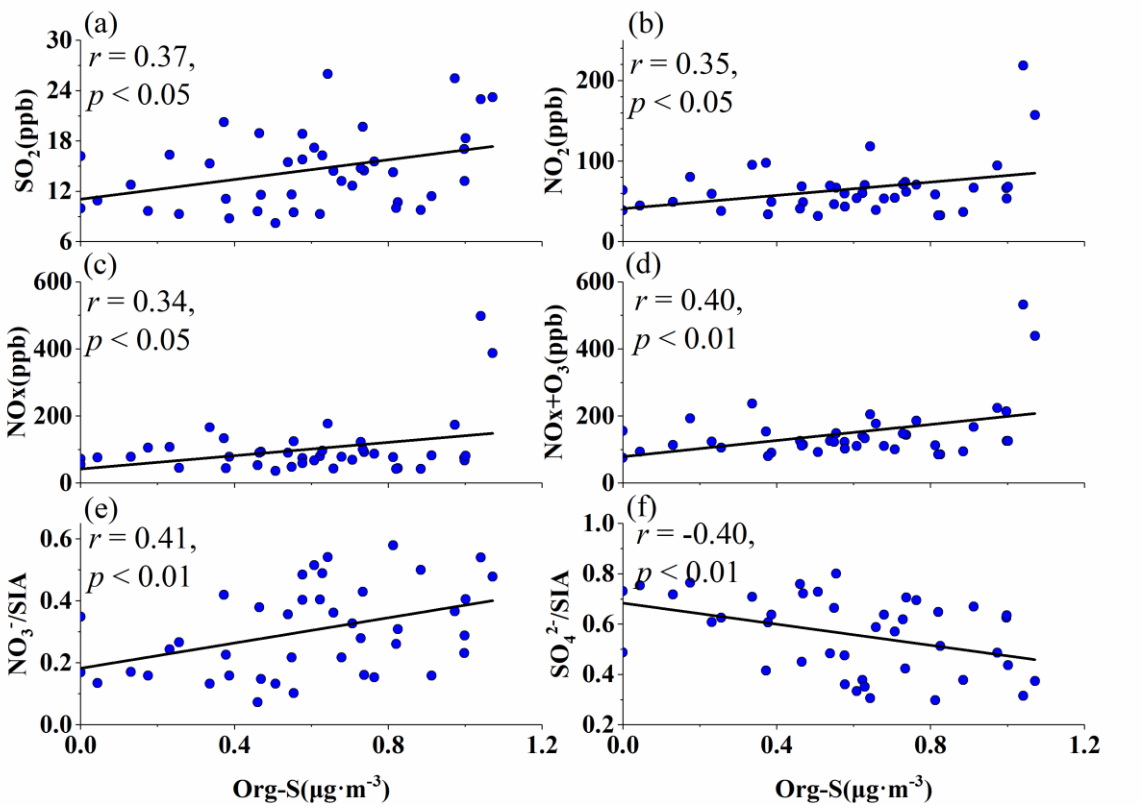

Figure S4. Significant correlations between the concentration of Org-S and (a) SO_2, (b) NO2, (c) NOx, (d) NOx+O_3, (e) NO_3^-/SIA, (f) SO_4^{2-}/SIA.

Table S1. Summary of the concentration of organosulfur (OrgS) and fraction in total particulate sulfur (TS), organic carbon (OC), organic matter (OM), and $PM_{2.5}$ mass reported in recent studies.

Sites		OrgS ($\mu g/m^3$)	OrgS/TS	OrgS /OC	OrgS /OM	OrgS /PM	Ref.
Guangzhou		0.04-1.1 (0.6)	0.07-50% (33%)		3.5-30% (14%)	0-3% (1.4%)	This study
Four Asian sites	Maldives	0.3 (OS)	2.1%	4.4%		0.9 %(OS)	(Stone et al., 2012)
	Gosan	0.1 (OS)	1.1%	3.5%		0.6% (OS)	
	Singapore	0.3 (OS)	2.5%			1.4% (OS)	
	Lahore	0.9-2 (OS)	5.9-7.7%	0.4-0.8%		0.7-0.9% (OS)	
Continental aerosol						4% (OS)	(Hawkins et al., 2010)
Whistler, British Columbia						< 1%(OS)	(Schwartz et al., 2010)
Polar region			6%		9-11%		(Frossard et al., 2011)
Kpuszta, Hungary		0.02-0.09	6-12%		8-50 %(OS)		(Luk´Acs et al., 2009)
		0.33	20%		30 %(OS)		(Surratt et al., 2008)
Fairbanks, Alaska				1.3%		0.8%	(Shakya and Peltier, 2013)
				0.7-2.1% (OS)		0.6-1.0% (OS)	
Eight sites in U.S.		up to 0.07		10-13%		1-3%	(Shakya and Peltier, 2015)
12 sites in U.S.		0.1-1.4		1-20% (OS)	5-10% (OS)		(Tolocka and Turpin, 2012)
Mt Kleiner Feldberg in central Germany			40%				(Vogel et al., 2016)
21 sites in U.S.		<0.0376 to 0.3					(Dombek et al., 2020)
U.S. (eastern and western, composite)		0.3±0.2 to 0.5±0.2	16±3 to 17±5				(Chen et al., 2021)

Table S2. Summary of the calculated molecular characteristics of organosulfur compounds groups detected in the yearlong sample set.

		For sample										For SOC formulas set	
Group	Subgroup	Number of formulas	% of total SOC formulas	% of total SOC abundance	Number of formulas with $o/(4s+3n) \geq 1$	% of formulas with $o/(4s+3n) \geq 1$	MW	H/C	O/C	O/S	DBE	Number of formulas	% of formulas with o/(4s+3n) ≥ 1
CHOS	$CHOS_1$	406-2199	57(50-67)	70(56-80)	389-2143	97(94-99)	349(305-378)	1.78(1.72-1.84)	0.52(0.40-0.67)	6.7(5.8-7.7)	2.64(2.22-2.90)	5664	5256(93%)
	$CHOS_2$	82-291	6(4-12)	2(1-6)	35-149	46(31-63)	583(519-649)	1.50(1.30-1.66)	0.33(0.21-0.50)	3.8(3-4.3)	7.80(5.78-9.38)	3722	2017(54%)
	Total	**498-2383**	**64(58-73)**	**72(59-84)**	**432-2262**	**92(87-95)**	**355(315-389)**	**1.77(1.72-1.83)**	**0.52(0.40-0.68)**	**6.7(5.7-7.7)**	**2.77(2.39-3.50)**	**9386**	**7273(77%)**
CHONS	$CHON_1S$	190-1344	31(22-35)	26(15-37)	159-1177	83(75-89)	366(325-399)	1.72(1.65-1.77)	0.71(0.63-0.84)	8.4(7.5-9.5)	3.46(3.10-4.45)	4397	3253(74%)
	$CHON_2S$	40-247	5(2-10)	2(1-6)	25-227	78(48-94)	455(390-553)	1.69(1.42-1.80)	0.90(0.61-1.35)	11.0(9.7-11.9)	4.85(3.49-8.06)	2215	1357(61%)
	Total	**269-1591**	**36(27-42)**	**28(16-41)**	**202-1389**	**82(70-89)**	**373(331-405)**	**1.72(1.62-1.76)**	**0.72(0.63-0.85)**	**8.6(7.7-9.7)**	**3.56(3.15-4.89)**	**6612**	**4610(70%)**

Table S3. Comparison of O/C and H/C ratios of CHOS compounds in this study and other studies.

Sample/type	Site/type		Extraction solution	O/C	H/C	Instrument	Ref.
$PM_{2.5}$	CHOS		Methanol	0.52±0.07	1.77±0.03	FT-ICR MS	This study
Rainwater	Northeastern United States		Water	1.3±0.8	1.9±0.5	FT-ICR MS	(Altieri et al., 2009)
$PM_{2.5}$	Pearl River Delta		Water	0.55 ± 0.17	1.67±0.31	Orbitrap MS	(Lin et al., 2012a)
$PM_{2.5}$	Cambridge	winter summer	Water and acetonitrile	0.47 0.66	1.47 1.50	Orbitrap MS	(Rincón et al., 2012)
Cloud	Colorado		Water	0.43±0.09 0.42±0.05	1.41±0.27 1.41±0.17	FT-ICR MS	(Zhao et al., 2013)
PM (0.18-1.8 μm)	California	after midnight morning afternoon before midnight		0.87±0.09 0.93±0.1 0.82±0.09 0.88±0.05	1.7±0.05 1.8±0.1 1.8±0.05 1.8±0.0	Orbitrap MS	(O'brien et al., 2014)
TSP	Virginia		Water Pyridine Acetonitrile	0.47±0.23 0.49±0.31 0.49±0.32	1.46±0.35 1.54±0.38 1.42±0.36	FT-ICR MS	(Willoughby et al., 2014)
$PM_{2.5}$	Beijing	Hazy Clear Hazy Clear	DCM DCM Water Water	0.49±0.26 0.62±0.34 0.65±0.28 0.75±0.37	1.55±0.41 1.74±0.34 1.64±0.37 1.82±0.26	FT-ICR MS	(Jiang et al., 2016)
$PM_{2.5}$	Wuhan Nanjing Shanghai	Winter Summer Summer Winter Summer	Methanol	0.37±0.25 0.39±0.23 0.43±0.32 0.40±0.29 0.47±0.31	1.68±0.44 1.75±0.36 1.68±0.41 1.68±0.46 1.68±0.42	Orbitrap MS	(Wang et al., 2016)
$PM_{2.5}$	Shanghai	Spring Summer Fall Winter	Acetonitrile	0.2 0.6 0.4 0.2	1 1.1 1.2 1.3	Orbitrap MS	(Wang et al., 2017)
$PM_{2.5}$	Mainz	low-pollution	Acetonitrile-water	0.78	1.66	Orbitrap MS	(Wang et al., 2018)

Cloud	Beijing	low-pollution	Water	0.63	1.81	FT-ICR MS	(Bianco et al., 2018)
		high-pollution		0.51	1.74		
	France			0.3	1.52		
$PM_{2.5}$	Changchun		Acetonitrile water	1.17±0.13	1.56±0.11	Orbitrap MS	(Wang et al., 2021)
	Shanghai			1.41±0.19	1.85±0.04		
	Guangzhou			1.48±0.05	1.85±0.02		

Table S4. Comparison of O/C and H/C ratios of CHONS compounds in this study and other studies.

Sample/type	Site/type		Extraction solution	O/C	H/C	Instrument	Ref.
$PM_{2.5}$	CHONS		Methanol	0.72±0.06	1.72±0.03	FT-ICR MS	This study
rainwater	Northeastern United States		Water	1.7 ±0.9	1.8 ±0.6	FT-ICR MS	(Altieri et al., 2009)
$PM_{2.5}$	Pearl River Delta		Water	0.81 ± 0.22	1.73 ± 0.29	Orbitrap MS	(Lin et al., 2012a)
$PM_{2.5}$	Cambridge	winter summer	Water and acetonitrile	0.73 0.80	1.99 1.65	Orbitrap MS	(Rincón et al., 2012)
Cloud	Colorado		Water	0.44±0.04 0.43±0.04	1.17±0.10 1.19±0.11	FT-ICR MS	(Zhao et al., 2013)
PM (0.18-1.8 μm)	California	after midnight morning afternoon before midnight		0.99±0.02 1.0±0.005 0.92±0.03 0.89±0.09	1.7±0.0 1.7±0.0 1.7±0.05 1.7±0.05	Orbitrap MS	(O'brien et al., 2014)
TSP	Virginia		Water Pyridine Acetonitrile	0.71±0.21 0.64±0.23 0.45±0.25	1.65±0.20 1.52±0.28 1.27±0.29	FT-ICR MS	(Willoughby et al., 2014)
$PM_{2.5}$	Beijing	Hazy Clear Hazy Clear	DCM Water	0.69±0.31 0.76±0.27 0.70±0.32	1.57±0.37 1.75±0.31 1.51±0.37	FT-ICR MS	(Jiang et al., 2016)
$PM_{2.5}$	Nanjing	Summer	Methanol	0.44±0.21	1.69±0.35	Orbitrap MS	(Wang et al., 2016)
	Wuhan	Winter Summer		0.35±0.13 0.40±0.17	1.58±0.46 1.69±0.34		
	Shanghai	Winter Summer		0.42±0.27 0.53±0.38	1.64±0.52 1.64±0.47		
$PM_{2.5}$	Shanghai	Spring Summer Fall Winter	Acetonitrile	0.2 0.4 0.3 0.4	1.5 1.5 1.6 1.5	Orbitrap MS	(Wang et al., 2017)
$PM_{2.5}$	Mainz	low-pollution	Acetonitrile-water	0.91	1.54	Orbitrap MS	(Wang et al., 2018)

Cloud	Beijing	low-pollution	Water	0.81	1.57	FT-ICR MS	(Bianco et al., 2018)
		high-pollution		0.59	1.56		
	France			0.23	1.47		
$PM_{2.5}$	Changchun		Acetonitrile-water	1.07±0.11	1.35±0.02	Orbitrap MS	(Wang et al., 2021)
	Shanghai			1.00±0.13	1.56±0.03		
	Guangzhou			0.82±0.03	1.56±0.04		

Table S5. Summary of the calculated molecular characteristics of organosulfur compounds groups detected in source samples, as the FT-ICR MS data are obtained from Cui et al. (2019) and Tang et al. (2020)

		Formula number	MW	H/C	O/C	O/S	DBE	% of (DBE-N) ⩾4	% of Xc⩾2.5	% of $o/(4s+3n) \geq 1$
BBOA1(Musa)	CHOS	444	360	1.52	0.47	6.21	4.76	57	43	88
	CHONS	371	379	1.55	0.50	7.21	4.98	58	64	64
	Avg/total	815	367	1.53	0.48	6.59	4.85	57	53	77
BBOA2(Hevea)	CHOS	174	396	1.35	0.40	5.97	7.68	69	59	86
	CHONS	65	411	1.56	0.50	7.51	4.79	62	69	63
	Avg/total	239	400	1.40	0.42	6.34	6.98	67	62	80
CCOA1(Anthracite)	CHOS	549	323	1.01	0.40	5.40	8.55	85	82	95
	CHONS	767	340	0.98	0.52	6.49	8.99	94	97	47
	Avg/total	1316	332	0.99	0.47	6.03	8.80	90	91	67
CCOA2(Bituminous coal)	CHOS	463	340	0.99	0.31	4.64	9.90	96	94	85
	CHONS	293	308	0.97	0.49	5.82	8.04	92	93	29
	Avg/total	756	328	0.98	0.38	5.10	9.18	94	93	63
Vehicle emissions	CHOS	112	441	1.31	0.25	4.47	9.54	71	71	75
	CHONS	17	400	1.17	0.72	8.59	6.92	59	59	47
	Avg/total	129	432	1.28	0.35	5.36	8.97	69	69	71
Tunnel aerosols	CHOS	635	325	1.74	0.59	6.79	2.75	46	23	96
	CHONS	410	340	1.81	0.90	8.73	2.78	28	29	91
	Avg/total	1045	331	1.76	0.71	7.53	2.76	39	25	94
Excavator-idling(diesel)	CHOS	1004	353	1.61	0.38	5.81	4.18	68	58	96
	CHONS	310	325	1.47	0. 41	5.59	5.18	56	65	42
	Avg/total	1314	347	1.59	0.38	5.77	4.38	65	60	83
Excavator-moving(diesel)	CHOS	334	326	1.51	0.46	5.20	3.58	54	49	98
	CHONS	117	298	1.62	0.48	5.17	5.55	59	64	9
	Avg/total	451	314	1.35	0.42	5.19	4.38	56	53	75
Excavator-working(diesel)	CHOS	631	342	1.63	0.36	5.44	4.00	62	55	93
	CHONS	260	323	1.47	0.40	5.41	5.26	62	69	27
	Avg/total	891	337	1.58	0.37	5.19	4.35	62	59	74
Diesel-vessels	CHOS	334	306	1.66	0.40	5.14	3.47	55	50	95
	CHONS	13	461	1.50	0.36	6.74	9.38	38	38	46
	Avg/total	347	310	1.66	0.40	5.17	3.60	54	49	93
Heavy-fuel-oil-vessels	CHOS	1110	311	1.48	0.36	4.77	4.85	76	71	83
	CHONS	398	343	1.35	0.39	5.68	6.35	80	86	28
	Avg/total	1508	314	1.47	0.36	4.86	5.00	77	75	68

Table S6. Detailed relative abundance of isoprene-derived OSs detected at Guangzhou. Noted the formulas in the Table S6-S10 were from the summarization of recent studies and the reference in (Bruggemann et al., 2020; Ye et al., 2020; Zhu et al., 2019; Wang et al., 2019).

Formula [M-H]$^-$	MW (Da)	DBE	Average RI (‰)
C4H5O5S–	164.9863	2	0.019
C4H7O5S–	167.0020	1	0.067
C3H5O6S–	168.9812	1	0.093
C3H7O6S–	170.9969	0	0.106
C4H5O6S–	180.9812	2	0.049
C5H9O5S–	181.0176	1	0.109
C4H7O6S–	182.9969	1	0.145
C3H5O7S–	184.9761	1	0.200
C5H7O6S–	194.9969	2	0.179
C5H9O6S–	197.0125	1	0.366
C3H3O8S–	198.9554	2	0.372
C4H7O7S–	198.9918	1	0.169
C5H11O6S–	199.0282	0	0.191
C3H5O8S–	200.9711	1	0.192
C5H7O7S–	210.9918	2	0.752
C5H9O7S–	213.0074	1	0.482
C4H7O8S–	214.9867	1	0.119
C5H11O7S–	215.0231	0	0.141
C3H5O9S–	216.9660	1	0.100
C7H9O6S–	221.0125	3	0.106
C8H13O5S–	221.0489	2	0.167
C5H7O8S–	226.9867	2	0.509
C5H9O8S–	229.0024	1	0.170
C4H7O9S–	230.9816	1	0.062
C5H11O8S–	231.0180	0	0.030
C8H11O6S–	235.0282	3	0.175
C7H9O7S–	237.0074	3	0.703
C8H13O6S–	237.0438	2	1.079
C8H11O7S–	251.0231	3	0.789
C8H13O7S–	253.0387	2	2.206
C9H15O7S–	267.0544	2	1.512
C8H13O8S–	269.0337	2	0.579
C5H7O11S–	274.9715	2	0.036
C12H19O6S–	291.0908	3	0.206
C8H13O10S–	301.0235	2	0.061
C12H17O8S–	321.0650	4	0.139
C10H19O10S–	331.0704	1	0.028
C10H21O10S–	333.0861	0	0.070
C15H31O13S–	451.1491	0	0.035
C5H10NO8S–	244.0133	1	0.172
C5H10NO9S–	260.0082	1	0.230
C5H8NO10S–	273.9874	2	0.099
C5H9N2O11S–	304.9933	2	0.108
C8H12NO12S–	346.0086	3	0.039

Table S7. Detailed relative abundance of terpene-derived OSs (including limonene) detected at Guangzhou.

Formula [M-H] $^-$	MW (Da)	DBE	Average RI (‰)
C6H11O4S–	179.0384	1	0.055
C5H11O6S–	199.0282	0	0.166
C3H5O8S–	200.9711	1	0.167
C6H11O6S–	211.0282	1	0.348
C5H11O7S–	215.0231	0	0.431
C9H15O4S–	219.0697	2	0.169
C9H17O4S–	221.0853	1	0.189
C7H11O6S–	223.0282	2	0.291
C9H19O4S–	223.1010	0	0.391
C7H13O6S–	225.0438	1	0.462
C5H7O8S–	226.9867	2	0.503
C5H9O8S–	229.0024	1	0.469
C9H9O5S–	229.0176	5	0.471
C10H13O4S–	229.0540	4	0.478
C10H15O4S–	231.0697	3	0.453
C9H15O5S–	235.0646	2	0.252
C8H13O6S–	237.0438	2	0.403
C10H21O4S–	237.1166	0	0.478
C10H9O5S–	241.0176	6	0.630
C8H17O6S–	241.0751	0	0.669
C6H11O8S–	243.0180	1	0.656
C9H9O6S–	245.0125	5	0.279
C10H15O5S–	247.0646	3	0.129
C9H13O6S–	249.0438	3	0.140
C10H17O5S–	249.0802	2	0.217
C7H7O8S–	250.9867	4	0.236
C8H11O7S–	251.0231	3	0.326
C9H15O6S–	251.0595	2	0.507
C10H19O5S–	251.0959	1	0.771
C7H9O8S–	253.0024	3	0.793
C8H13O7S–	253.0387	2	0.912
C9H17O6S–	253.0751	1	1.038
C10H21O5S–	253.1115	0	1.056
C9H7O7S–	258.9918	6	0.416
C10H11O6S–	259.0282	5	0.290
C10H13O6S–	261.0438	4	0.062
C9H11O7S–	263.0231	4	0.080
C10H15O6S–	263.0595	3	0.153
C8H9O8S–	265.0024	4	0.189
C9H13O7S–	265.0387	3	0.352
C10H17O6S–	265.0751	2	0.480
C8H11O8S–	267.0180	3	0.613
C9H15O7S–	267.0544	2	0.799
C10H19O6S–	267.0908	1	0.910
C9H17O7S–	269.0700	1	0.899
C7H11O9S–	271.0129	2	0.751
C10H9O7S–	273.0074	6	0.313
C8H17O8S–	273.0650	0	0.186
C10H15O7S–	279.0544	3	0.443
C9H13O8S–	281.0337	3	0.768
C10H17O7S–	281.0700	2	0.986
C12H11O6S–	283.0282	7	1.001

C9H15O8S–	283.0493	2	1.067
C10H19O7S–	283.0857	1	1.150
C8H13O9S–	285.0286	2	0.826
C11H15O7S–	291.0544	4	0.089
C9H11O9S–	295.0129	4	0.475
C10H15O8S–	295.0493	3	0.595
C9H13O9S–	297.0286	3	0.737
C10H17O8S–	297.0650	2	0.834
C9H15O9S–	299.0442	2	0.580
C14H23O5S–	303.1272	3	0.137
C11H17O8S–	309.0650	3	0.477
C10H15O9S–	311.0442	3	0.642
C10H17O9S–	313.0599	2	0.478
C15H25O5S–	317.1428	3	0.106
C14H23O6S–	319.1221	3	0.152
C10H15O10S–	327.0391	3	0.358
C14H21O7S–	333.1013	4	0.129
C15H25O6S–	333.1377	3	0.164
C10H13O11S–	341.0184	4	0.411
C15H23O7S–	347.1170	4	0.136
C14H21O8S–	349.0963	4	0.206
C14H23O8S–	351.1119	3	0.305
C15H23O8S–	363.1119	4	0.188
C16H27O7S–	363.1483	3	0.235
C16H27O8S–	379.1432	3	0.321
C20H31O5S–	383.1898	5	0.240
C20H33O5S–	385.2054	4	0.074
C20H33O9S2–	481.1571	4	0.061
C10H16NO7S–	294.0653	3	1.416
C9H14NO8S–	296.0446	3	1.483
C10H16NO8S–	310.0602	3	0.130
C9H14NO9S–	312.0395	3	0.178
C10H16NO9S–	326.0551	3	0.164
C10H18NO9S–	328.0708	2	0.274
C9H16NO10S–	330.0500	2	0.295
C10H16NO10S–	342.0500	3	0.212
C10H15N2O10S–	355.0453	4	0.153
C15H24NO7S–	362.1279	4	0.097
C10H17N2O11S–	373.0559	3	0.201
C14H24NO9S–	382.1177	3	0.131
C10H17N2O12S–	389.0508	3	0.066

Table S8. Detailed relative abundance of other biogenic VOCs-derived OSs (2-Methyl-3-Buten-2-ol; 2-E-pentenal, 2-E-hexenal, 3-Z-hexenal, and cis-3-hexen-1-ol, β-caryophyllene) detected at Guangzhou.

Formula $[M-H]^-$	MW (Da)	DBE	Average RI (‰)
C3H5O6S–	168.9812	1	0.060
C4H9O5S–	169.0176	0	0.069
C3H5O7S–	184.9761	1	0.142
C5H11O6S–	199.0282	0	0.264
C6H9O6S–	209.0125	2	0.219
C6H11O6S–	211.0282	1	0.607
C5H9O7S–	213.0074	1	0.630

C5H9O8S–	229.0024	1	0.387
C9H15O6S–	251.0595	2	0.790
C9H17O7S–	269.0700	1	0.910
C14H23O5S–	303.1272	3	0.140
C15H25O5S–	317.1428	3	0.110
C14H23O6S–	319.1221	3	0.199
C14H21O7S–	333.1013	4	0.191
C15H25O6S–	333.1377	3	0.201
C15H23O7S–	347.1170	4	0.190
C14H21O8S–	349.0963	4	0.135
C14H23O8S–	351.1119	3	0.336
C15H23O8S–	363.1119	4	0.237
C16H27O7S–	363.1483	3	0.289
C16H27O8S–	379.1432	3	0.419
C15H24NO7S–	362.1279	4	0.162
C14H24NO9S–	382.1177	3	0.151

Table S9. Detailed relative abundance of anthropogenic VOCs-derived OSs detected at Guangzhou.

Formula [M-H]$^-$	MW (Da)	DBE	Average RI (‰)
C6H5O4S–	172.9914	4	0.060
C7H5O4S–	184.9914	5	0.109
C7H7O4S–	187.0071	4	0.120
C5H7O6S–	194.9969	2	0.108
C8H7O4S–	199.0071	5	0.213
C7H5O5S–	200.9863	5	0.216
C8H9O4S–	201.0227	4	0.214
C6H9O6S–	209.0125	2	0.169
C7H13O5S–	209.0489	1	0.243
C8H7O5S–	215.0020	5	0.506
C9H11O4S–	215.0384	4	0.358
C8H5O6S–	228.9812	6	0.597
C9H9O5S–	229.0176	5	0.574
C9H11O5S–	231.0333	4	0.164
C9H17O5S–	237.0802	1	0.624
C10H19O5S–	251.0959	1	1.026
C10H17O6S–	265.0751	2	0.623
C9H15O7S–	267.0544	2	1.043
C9H17O7S–	269.0700	1	0.986
C10H9O7S–	273.0074	6	0.234
C10H11O7S–	275.0231	5	0.049
C12H23O5S–	279.1272	1	0.830
C10H17O7S–	281.0700	2	1.192
C9H17O8S–	285.0650	1	0.473
C11H11O7S–	287.0231	6	0.312
C11H13O7S–	289.0387	5	0.062
C10H15O8S–	295.0493	3	0.651
C10H17O8S–	297.0650	2	0.669
C6H4NO6S–	217.9765	5	0.061
C10H10NO9S–	320.0082	6	0.040
C10H16NO9S–	326.0551	3	0.196

Table S10. Detailed relative abundance of OSs derived from precursors of multiple sources detected at Guangzhou, including Methyl Vinyl, Methacrolein, glyoxal, methylglyoxal, Oleic acid, and other unsaturated acids, such as Palmitoleic acid, Linoleic acid, Conjugated linoleic acid, 10-Undecenoic acid, as well as some alkanes such as 1-Dodecene.

Formula [M-H]$^-$	MW (Da)	DBE	Average RI (‰)
C3H7O5S–	155.0020	0	0.087
C4H5O5S–	164.9863	2	0.076
C4H7O5S–	167.0020	1	0.588
C3H5O6S–	168.9812	1	0.127
C5H7O5S–	179.0020	2	0.144
C5H9O5S–	181.0176	1	0.719
C4H7O6S–	182.9969	1	0.683
C5H7O6S–	194.9969	2	0.907
C6H11O5S–	195.0333	1	1.546
C5H9O6S–	197.0125	1	1.113
C3H3O8S–	198.9554	2	0.004
C3H5O8S–	200.9711	1	0.015
C6H7O6S–	206.9969	3	0.312
C7H11O5S–	207.0333	2	0.487
C8H15O4S–	207.0697	1	0.392
C6H9O6S–	209.0125	2	2.961
C7H13O5S–	209.0489	1	2.110
C8H17O4S–	209.0853	0	2.239
C5H7O7S–	210.9918	2	1.181
C6H11O6S–	211.0282	1	2.907
C7H15O5S–	211.0646	0	0.858
C5H9O7S–	213.0074	1	0.565
C4H7O8S–	214.9867	1	0.002
C3H5O9S–	216.9660	1	0.017
C8H13O5S–	221.0489	2	0.742
C9H17O4S–	221.0853	1	0.344
C8H15O5S–	223.0646	1	3.136
C9H19O4S–	223.1010	0	0.657
C5H9O8S–	229.0024	1	0.084
C4H7O9S–	230.9816	1	0.007
C9H15O5S–	235.0646	2	5.496
C10H19O4S–	235.1010	1	0.431
C7H9O7S–	237.0074	3	1.350
C8H13O6S–	237.0438	2	4.505
C9H17O5S–	237.0802	1	2.513
C8H15O6S–	239.0595	1	4.788
C5H9O9S–	244.9973	1	0.006
C10H17O5S–	249.0802	2	2.914
C11H21O4S–	249.1166	1	0.448
C9H15O6S–	251.0595	2	6.871
C10H19O5S–	251.0959	1	10.186
C9H17O6S–	253.0751	1	4.825
C8H15O7S–	255.0544	1	1.826
C9H19O6S–	255.0908	0	0.549
C10H17O6S–	265.0751	2	4.866
C11H21O5S–	265.1115	1	3.640
C8H11O8S–	267.0180	3	2.195

C9H15O7S–	267.0544	2	7.408
C10H19O6S–	267.0908	1	4.505
C9H17O7S–	269.0700	1	2.203
C8H15O8S–	271.0493	1	0.394
C5H7O11S–	274.9715	2	0.006
C13H25O4S–	277.1479	1	0.545
C10H15O7S–	279.0544	3	9.100
C11H19O6S–	279.0908	2	3.420
C12H23O5S–	279.1272	1	4.561
C11H21O6S–	281.1064	1	3.002
C10H19O7S–	283.0857	1	2.828
C9H17O8S–	285.0650	1	0.564
C12H19O6S–	291.0908	3	1.309
C12H21O6S–	293.1064	2	2.970
C13H25O5S–	293.1428	1	5.245
C10H15O8S–	295.0493	3	4.782
C10H17O8S–	297.0650	2	3.585
C11H21O7S–	297.1013	1	1.343
C10H19O8S–	299.0806	1	1.084
C9H17O9S–	301.0599	1	0.076
C14H23O5S–	303.1272	3	0.671
C14H25O5S–	305.1428	2	1.476
C15H29O4S–	305.1792	1	0.614
C14H27O5S–	307.1585	1	6.946
C15H31O4S–	307.1949	0	1.458
C13H25O6S–	309.1377	1	2.465
C15H25O5S–	317.1428	3	0.720
C14H23O6S–	319.1221	3	1.328
C15H27O5S–	319.1585	2	1.399
C14H25O6S–	321.1377	2	2.457
C15H29O5S–	321.1741	1	7.015
C14H27O6S–	323.1534	1	2.529
C15H31O5S–	323.1898	0	0.906
C13H25O7S–	325.1326	1	1.016
C14H21O7S–	333.1013	4	1.254
C15H25O6S–	333.1377	3	1.362
C16H29O5S–	333.1741	2	1.408
C15H27O6S–	335.1534	2	2.050
C16H31O5S–	335.1898	1	6.059
C14H25O7S–	337.1326	2	2.532
C15H29O6S–	337.1690	1	2.283
C16H33O5S–	337.2054	0	1.863
C15H23O7S–	347.1170	4	1.842
C17H31O5S–	347.1898	2	1.309
C14H21O8S–	349.0963	4	1.610
C15H25O7S–	349.1326	3	2.194
C16H29O6S–	349.1690	2	2.253
C14H23O8S–	351.1119	3	2.031
C15H27O7S–	351.1483	2	2.370
C16H31O6S–	351.1847	1	5.103
C14H25O8S–	353.1276	2	1.433
C15H29O7S–	353.1639	1	1.019
C18H31O5S–	359.1898	3	0.433

C18H33O5S–	361.2054	2	1.181
C15H23O8S–	363.1119	4	1.893
C16H27O7S–	363.1483	3	1.767
C17H31O6S–	363.1847	2	1.538
C18H35O5S–	363.2211	1	3.739
C16H29O7S–	365.1639	2	3.434
C17H33O6S–	365.2003	1	3.154
C15H27O8S–	367.1432	2	1.283
C18H31O6S–	375.1847	3	0.767
C18H33O6S–	377.2003	2	1.728
C19H37O5S–	377.2367	1	2.472
C16H27O8S–	379.1432	3	1.754
C18H35O6S–	379.2160	1	2.906
C16H29O8S–	381.1589	2	1.390
C15H15O10S–	387.0391	8	0.037
C20H37O5S–	389.2367	2	0.666
C18H31O7S–	391.1796	3	1.175
C19H35O6S–	391.2160	2	1.002
C20H39O5S–	391.2524	1	1.834
C18H33O7S–	393.1952	2	2.059
C17H31O8S–	395.1745	2	1.121
C18H35O7S–	395.2109	1	2.020
C20H37O6S–	405.2316	2	0.823
C21H41O5S–	405.2680	1	1.159
C18H31O8S–	407.1745	3	1.129
C18H33O8S–	409.1902	2	1.211
C22H41O5S–	417.2680	2	0.406
C22H43O5S–	419.2837	1	0.879
C22H41O6S–	433.2629	2	0.466
C23H45O5S–	433.2993	1	0.859
C24H45O6S–	461.2942	2	0.342
C24H47O6S–	463.3099	1	0.925
C24H45O7S–	477.2891	2	0.426
C5H8NO8S–	241.9976	2	0.591
C6H12NO8S–	258.0289	1	1.249
C10H16NO9S–	326.0551	3	3.361
C9H16NO10S–	330.0500	2	0.461
C15H24NO7S–	362.1279	4	2.253
C14H24NO9S–	382.1177	3	0.923

Table S11. Number and percentage occurrences of the plausible reactant− product pairs

Type	Number			Percentage		
	Median	Range	Average± STD	Median	Range	Average± STD
CHOS − SO3 → CHO (1)	708	87-1249	699±324	28	11-37	27±7
CHONS − SO3 → CHON (2)	480	48-971	508±261	20	5-27	19±6
Total	1158	135-2165	1207±578	48	18-62	46±12

Table S12. Selected meteorological parameters and chemical variables that probably have influences on the formation of NOCs. This table has been revised from our previous study and the references therein (Jiang et al., 2021b).

Abbreviation	Full name	Major Sources/influences
SO_2	Sulfur dioxide	Combustion sources
NO	Nitric oxide	
NO_2	Nitrogen dioxide	
NOx	Nitrogen oxides	
CO	Carbon monoxide	
O_3	Ozone	Photo-oxidization
NOx+ O_3	Oxidants	
NH_4^+	Ammonium	Secondary nitrate formation process
NO_3^-	Nitrates	
SO_4^{2-}/nss-SO_4^{2-}	Sulfates/ non-sea-salt sulfates	Secondary sulfate formation process
Cl^-	Chloridion	Sea salt/coal conbustion
K^+/nss-K^+	Potassium/non-sea-salt potassium	Biomass burning (also from coal combustion and other sources)
Levo	levoglucosan	Biomass burning
MTLs	sum of 2-methylthreitol and 2-methylerythritol	Isoprene derived SOA
MSOA	monoterpene-derived secondary organic aerosols	α -/β-pinene derived SOA
FA	Fatty acids	Vehicle emission, coal combustion, cooking, high-level plans
PAHs	Polycyclic aromatic hydrocarbons	Combustion sources
Alkane	Long-chain alkanes with C number from 20 to 36	Combustion sources and high-level plans
ΣSH	steranes and hopanes	Fossil fuels combustion sources
LWC	Liquid water content	Influence the aqueous phase reaction
Tem	Temperature	Influence the gas-to-particle partitioning
RH	Relative humidity	Influence the aqueous phase reaction
OH	Hydroxyl radical	Influence the oxidation state of precursor/ photo-decomposed
pH	potential of hydrogen	Influence the aqueous phase reaction (range: -0.08-4.90)
$\Delta^{14}C$	Radiocarbon isotope	Indicator of fossil or non-fossil sources

Table S13. Number and percentage of compounds classes with significant correlations to the environmental variables.

Type	*p*-value original				*p*-value (FDR-adjusted			
	CHOS		CHONS		CHOS		CHONS	
Parameters	Positive	Negative	Positive	Negative	Positive	Negative	Positive	Negative
RH	591 (77%)	172 (72%)	180 (23%)	66 (28%)	322 (83%)	20 (74%)	65 (17%)	7 (26%)
Tem	260 (83%)	697 (58%)	54 (17%)	514 (42%)	170 (89%)	352 (57%)	22 (11%)	261 (43)
MSOA	478 (53%)	465 (88%)	416 (47%)	62 (12%)	375 (58%)	260 (92%)	277 (42%)	22 (8%)

MTLs	336 (73%)	696 (72%)	124 (27%)	274 (28%)	253 (81%)	451 ()	60	123
$\Delta^{14}C$	199 (70%)	440 (69%)	87 (30%)	200 (31%)	37 (71%)	225 (71%)	15 (29%)	92 (29%)
NH_4^+	230 (43%)	244 (85%)	306 (57%)	42 (15%)	21 (26%)	56 (89%)	59 (74%)	7 (11%)
NO_3^-	283 (44%)	159 (79%)	359 (56%)	42 (21%)	46 (36%)	40 (75%)	83 (64%)	13 (25%)
LWC	330 (46%)	22 (72%)	392 (54%)	8 (28%)	17 (100%)	0	43 (100%)	0
pH	65 (56%)	11 (48%)	51 (44%)	12 (52%)	0	0	0	0
SO_4^{2-}	247 (72%)	131 (63%)	95 (28%)	76 (37%)	0	0	0	0

References

Altieri, K. E., Turpin, B. J., and and Seitzinger, S. P.: Oligomers, organosulfates, and nitrooxy organosulfates in rainwater identified by ultra-high resolution electrospray ionization FT-ICR mass spectrometry, Atmos. Chem. Phys., 2533-2542, doi:10.5194/acp-9-2533-2009, 2009.
Bianco, A., Deguillaume, L., Vaitilingom, M., Nicol, E., Baray, J. L., Chaumerliac, N., and Bridoux, M.: Molecular Characterization of Cloud Water Samples Collected at the Puy de Dome (France) by Fourier Transform Ion Cyclotron Resonance Mass Spectrometry, Environ. Sci. Technol., 52, 10275-10285, doi:10.1021/acs.est.8b01964, 2018.
Bruggemann, M., Xu, R., Tilgner, A., Kwong, K. C., Mutzel, A., Poon, H. Y., Otto, T., Schaefer, T., Poulain, L., Chan, M. N., and Herrmann, H.: Organosulfates in Ambient Aerosol: State of Knowledge and Future Research Directions on Formation, Abundance, Fate, and Importance, Environ. Sci. Technol., 54, 3767-3782, doi:10.1021/acs.est.9b06751, 2020.
Chen, Y., Dombek, T., Hand, J., Zhang, Z., Gold, A., Ault, A. P., Levine, K. E., and Surratt, J. D.: Seasonal Contribution of Isoprene-Derived Organosulfates to Total Water-Soluble Fine Particulate Organic Sulfur in the United States, ACS Earth Space Chem., 5, 2419-2432, doi:10.1021/acsearthspacechem.1c00102, 2021.
Cui, M., Li, C., Chen, Y., Zhang, F., Li, J., Jiang, B., Mo, Y., Li, J., Yan, C., Zheng, M., Xie, Z., Zhang, G., and Zheng, J.: Molecular characterization of polar organic aerosol constituents in off-road engine emissions using Fourier transform ion cyclotron resonance mass spectrometry (FT-ICR MS): implications for source apportionment, Atmos. Chem. Phys., 19, 13945-13956, doi:10.5194/acp-19-13945-2019, 2019.
Dombek, T., Poitras, E., Hand, J., Schichtel, B., Harrington, J. M., and Levine, K. E.: Total sulfur analysis of fine particulate mass on nylon filters by ICP–OES, Journal of Environmental Quality, 49, 762-768, doi:https://doi.org/10.1002/jeq2.20066, 2020.
Frossard, A. A., Shaw, P. M., Russell, L. M., Kroll, J. H., Canagaratna, M. R., Worsnop, D. R., Quinn, P. K., and Bates, T. S.: Springtime Arctic haze contributions of submicron organic particles from European and Asian combustion sources, Journal of Geophysical Research, 116, doi:10.1029/2010jd015178, 2011.
Hawkins, L. N., Russell, L. M., Covert, D. S., Quinn, P. K., and Bates, T. S.: Carboxylic acids, sulfates, and organosulfates in processed continental organic aerosol over the southeast Pacific Ocean during VOCALS-REx 2008, Journal of Geophysical Research, 115, doi:10.1029/2009jd013276, 2010.
Jiang, B., Kuang, B. Y., Liang, Y., Zhang, J., Huang, X. H. H., Xu, C., Yu, J. Z., and Shi, Q.: Molecular composition of urban organic aerosols on clear and hazy days in Beijing: a comparative study using FT-ICR MS, Environ. Chem., 13, 888-901, doi:10.1071/en15230, 2016.
Jiang, H., Li, J., Sun, R., Tian, C., Tang, J., Jiang, B., Liao, Y., Chen, C. E., and Zhang, G.: Molecular Dynamics and Light Absorption Properties of Atmospheric Dissolved Organic Matter, Environ. Sci. Technol., 55, 10268-10279, doi:10.1021/acs.est.1c01770, 2021a.
Jiang, H., Li, J., Chen, D., Tang, J., Cheng, Z., Mo, Y., Su, T., Tian, C., Jiang, B., Liao, Y., and Zhang, G.: Biomass burning organic aerosols significantly influence the light

absorption properties of polarity-dependent organic compounds in the Pearl River Delta Region, China, Environ. Int., 144, 106079, doi:10.1016/j.envint.2020.106079, 2020.
Jiang, H., Li, J., Sun, R., Liu, G., Tian, C., Tang, J., Cheng, Z., Zhu, S., Zhong, G., Ding, X., and Zhang, G.: Determining the Sources and Transport of Brown Carbon Using Radionuclide Tracers and Modeling, J. Geophys. Res. Atmos., 126, doi:10.1029/2021jd034616, 2021b.
Kuang, B. Y., Lin, P., Hu, M., and Yu, J. Z.: Aerosol size distribution characteristics of organosulfates in the Pearl River Delta region, China, Atmos. Environ., 130, 23-35, doi:10.1016/j.atmosenv.2015.09.024, 2016.
Lin, P., Rincon, A. G., Kalberer, M., and Yu, J. Z.: Elemental Composition of HULIS in the Pearl River Delta Region, China: Results Inferred from Positive and Negative Electrospray High Resolution Mass Spectrometric Data, Environmental Science & Technology, 46, 7454-7462, doi:10.1021/es300285d, 2012a.
Lin, P., Yu, J. Z., Engling, G., and Kalberer, M.: Organosulfates in Humic-like Substance Fraction Isolated from Aerosols at Seven Locations in East Asia: A Study by Ultra-High-Resolution Mass Spectrometry, Environ. Sci. Technol., 46, 13118-13127, doi:10.1021/es303570v, 2012b.
Luk´acs, H., Gelencs´er, A., Hoffer, A., Kiss, G., Horv´ath, K., and Harty´ani, Z.: Quantitative assessment of organosulfates in size-segregated rural fine aerosol, Atmos. Chem. Phys., 9, 231–238, doi:10.5194/acp-9-231-2009, 2009.
O'Brien, R. E., Laskin, A., Laskin, J., Rubitschun, C. L., Surratt, J. D., and Goldstein, A. H.: Molecular characterization of S- and N-containing organic constituents in ambient aerosols by negative ion mode high-resolution Nanospray Desorption Electrospray Ionization Mass Spectrometry: CalNex 2010 field study, J. Geophys. Res. Atmos., 119, 12706-12720, doi:10.1002/2014jd021955, 2014.
Rincón, A. G., Calvo, A. I., Dietzel, M., and and Kalberer, M.: Seasonal differences of urban organic aerosol composition – an ultra-high resolution mass spectrometry study, Environmental Chemistry, 9, 298-319, doi:10.1071/EN12016_AC, 2012.
Schwartz, R. E., Russell, L. M., Sjostedt, S. J., Vlasenko, A., Slowik, J. G., Abbatt, J. P. D., Macdonald, A. M., Li, S. M., Liggio, J., Toom-Sauntry, D., and Leaitch, W. R.: Biogenic oxidized organic functional groups in aerosol particles from a mountain forest site and their similarities to laboratory chamber products, Atmospheric Chemistry and Physics, 10, 5075-5088, doi:10.5194/acp-10-5075-2010, 2010.
Shakya, K. M. and Peltier, R. E.: Investigating missing sources of sulfur at Fairbanks, Alaska, Environ. Sci. Technol., 47, 9332-9338, doi:10.1021/es402020b, 2013.
Shakya, K. M. and Peltier, R. E.: Non-sulfate sulfur in fine aerosols across the United States: Insight for organosulfate prevalence, Atmos. Environ., 100, 159-166, doi:10.1016/j.atmosenv.2014.10.058, 2015.
Stone, E. A., Yang, L., Yu, L. E., and Rupakheti, M.: Characterization of organosulfates in atmospheric aerosols at Four Asian locations, Atmos. Environ., 47, 323-329, doi:10.1016/j.atmosenv.2011.10.058, 2012.
Surratt, J. D., Gómez-González, Y., Chan, A. W. H., Vermeylen, R., Shahgholi, M., Kleindienst, T. E., Edney, E. O., Offenberg, J. H., Lewandowski, M., Jaoui, M., Maenhaut, W., Claeys, M., Flagan, R. C., and Seinfeld, J. H.: Organosulfate Formation in Biogenic Secondary Organic Aerosol, J. Phys. Chem. A, 112, 8345-8378, doi:10.1021/jp802310p, 2008.

Tang, J., Li, J., Su, T., Han, Y., Mo, Y., Jiang, H., Cui, M., Jiang, B., Chen, Y., Tang, J., Song, J., Peng, P. a., and Zhang, G.: Molecular compositions and optical properties of dissolved brown carbon in biomass burning, coal combustion, and vehicle emission aerosols illuminated by excitation–emission matrix spectroscopy and Fourier transform ion cyclotron resonance mass spectrometry analysis, Atmos. Chem. Phys., 20, 2513-2532, doi:10.5194/acp-20-2513-2020, 2020.
Tolocka, M. P. and Turpin, B.: Contribution of organosulfur compounds to organic aerosol mass, Environ. Sci. Technol., 46, 7978-7983, doi:10.1021/es300651v, 2012.
Vogel, A. L., Schneider, J., Muller-Tautges, C., Phillips, G. J., Pohlker, M. L., Rose, D., Zuth, C., Makkonen, U., Hakola, H., Crowley, J. N., Andreae, M. O., Poschl, U., and Hoffmann, T.: Aerosol Chemistry Resolved by Mass Spectrometry: Linking Field Measurements of Cloud Condensation Nuclei Activity to Organic Aerosol Composition, Environ Sci Technol, 50, 10823-10832, doi:10.1021/acs.est.6b01675, 2016.
Wang, K., Zhang, Y., Huang, R.-J., Cao, J., and Hoffmann, T.: UHPLC-Orbitrap mass spectrometric characterization of organic aerosol from a central European city (Mainz, Germany) and a Chinese megacity (Beijing), Atmospheric Environment, 189, 22-29, doi:10.1016/j.atmosenv.2018.06.036, 2018.
Wang, K., Zhang, Y., Huang, R. J., Wang, M., Ni, H., Kampf, C. J., Cheng, Y., Bilde, M., Glasius, M., and Hoffmann, T.: Molecular Characterization and Source Identification of Atmospheric Particulate Organosulfates Using Ultrahigh Resolution Mass Spectrometry, Environ. Sci. Technol., 53, 6192-6202, doi:10.1021/acs.est.9b02628, 2019.
Wang, K., Huang, R.-J., Brüggemann, M., Zhang, Y., Yang, L., Ni, H., Guo, J., Wang, M., Han, J., Bilde, M., Glasius, M., and Hoffmann, T.: Urban organic aerosol composition in eastern China differs from north to south: molecular insight from a liquid chromatography–mass spectrometry (Orbitrap) study, Atmos. Chem. Phys., 21, 9089-9104, doi:10.5194/acp-21-9089-2021, 2021.
Wang, X., Hayeck, N., Brüggemann, M., Yao, L., Chen, H., Zhang, C., Emmelin, C., Chen, J., George, C., and Wang, L.: Chemical Characteristics of Organic Aerosols in Shanghai: A Study by Ultrahigh-Performance Liquid Chromatography Coupled With Orbitrap Mass Spectrometry, J. Geophys. Res. Atmos., 122, 11703-11722, doi:10.1002/2017jd026930, 2017.
Wang, X. K., Rossignol, S., Ma, Y., Yao, L., Wang, M. Y., Chen, J. M., George, C., and Wang, L.: Molecular characterization of atmospheric particulate organosulfates in three megacities at the middle and lower reaches of the Yangtze River, Atmos. Chem. Phys., 16, 2285–2298, doi:10.5194/acp-16-2285-2016, 2016.
Willoughby, A. S., Wozniak, A. S., and Hatcher, P. G.: A molecular-level approach for characterizing water-insoluble components of ambient organic aerosol particulates using ultrahigh-resolution mass spectrometry, Atmos. Chem. Phys., 14, 10299-10314, doi:10.5194/acp-14-10299-2014, 2014.
Yassine, M. M., Harir, M., Dabek-Zlotorzynska, E., and Schmitt-Kopplin, P.: Structural characterization of organic aerosol using Fourier transform ion cyclotron resonance mass spectrometry: aromaticity equivalent approach, Rapid Commun. Mass Spectrom., 28, 2445-2454, doi:10.1002/rcm.7038, 2014.
Ye, Y., Zhan, H., Yu, X., Li, J., Wang, X., and Xie, Z.: Detection of organosulfates and nitrooxy-organosulfates in Arctic and Antarctic atmospheric aerosols, using ultra-high

resolution FT-ICR mass spectrometry, Sci. Total Environ., 767, 144339, doi:10.1016/j.scitotenv.2020.144339, 2020.
Zhao, Y., Hallar, A. G., and Mazzoleni, L. R.: Atmospheric organic matter in clouds: exact masses and molecular formula identification using ultrahigh-resolution FT-ICR mass spectrometry, Atmos. Chem. Phys., 13, 12343-12362, doi:10.5194/acp-13-12343-2013, 2013.
Zhu, M., Jiang, B., Li, S., Yu, Q., Yu, X., Zhang, Y., Bi, X., Yu, J., George, C., Yu, Z., and Wang, X.: Organosulfur Compounds Formed from Heterogeneous Reaction between SO2 and Particulate-Bound Unsaturated Fatty Acids in Ambient Air, Environ. Sci. Technol. Lett., 6, 318-322, doi:10.1021/acs.estlett.9b00218, 2019.